TU Delft

Delft University of Technology

An Extended Linear Quadratic Model Predictive Control Approach for Multi-Destination Urban Traffic Networks

Han, Yu; Hegyi, Andreas; Yuan, Yufei; Roncoli, Claudio; Hoogendoorn, Serge

DOI
10.1109/TITS.2018.2877259

Publication date
2018

Document Version
Accepted author manuscript

Published in
IEEE Transactions on Intelligent Transportation Systems

Citation (APA)
Han, Y., Hegyi, A., Yuan, Y., Roncoli, C., & Hoogendoorn, S. (2018). An Extended Linear Quadratic Model Predictive Control Approach for Multi-Destination Urban Traffic Networks. *IEEE Transactions on Intelligent Transportation Systems*, *20 (2019)*(10), 3647-3660. https://doi.org/10.1109/TITS.2018.2877259

Important note
To cite this publication, please use the final published version (if applicable).
Please check the document version above.

Copyright
Other than for strictly personal use, it is not permitted to download, forward or distribute the text or part of it, without the consent of the author(s) and/or copyright holder(s), unless the work is under an open content license such as Creative Commons.

Takedown policy
Please contact us and provide details if you believe this document breaches copyrights.
We will remove access to the work immediately and investigate your claim.

This work is downloaded from Delft University of Technology.
For technical reasons the number of authors shown on this cover page is limited to a maximum of 10.

This article has been accepted for inclusion in a future issue of this journal. Content is final as presented, with the exception of pagination.

An Extended Linear Quadratic Model Predictive Control Approach for Multi-Destination Urban Traffic Networks

Yu Han, Andreas Hegyi, *Member, IEEE*, Yufei Yuan, Claudio Roncoli, and Serge Hoogendoorn

***Abstract*— This paper extends an existing linear quadratic model predictive control (LQMPC) approach to multi-destination traffic networks, where the correct origin–destination (OD) relations are preserved. In the literature, the LQMPC approach has been presented for efficient routing and intersection signal control. The optimization problem in the LQMPC has a linear quadratic formulation that can be solved quickly, which is beneficial for a real-time application. However, the existing LQMPC approach does not preserve OD relations and thus may send traffic to wrong destinations. This problem is tackled by a heuristic method presented is this paper. We present two macroscopic models: 1) a non-linear route-specific model which keeps track of traffic dynamics for each OD pair and 2) a linear model that aggregates all route traffic states, which can be embedded into the LQMPC framework. The route-specific model predicts traffic dynamics and provides information to the LQMPC before the optimization and evaluates the optimal solutions after the optimization. The information obtained from the route-specific model is formulated as constraints in the LQMPC to narrow the solution space and exclude unrealistic solutions that would lead to flows that are inconsistent with the OD relations. The extended LQMPC approach is tested in a synthetic network with multiple bottlenecks. The simulation of the LQMPC approach achieves a total time spent close to the system optimum, and the computation time remains tractable.**

***Index Terms*— Model predictive control, route guidance, signal control, linear model, spillback.**

I. Introduction

DUE to growing transportation demands and the urbanization trend, traffic congestion has become a global issue that has a significant impact on our society's productivity. Expanding the current infrastructure is not always viable due to high costs. Dynamic traffic control is an effective way to make better use of existing infrastructure. In urban traffic networks, traffic signal control strategies play an important role to improve the traffic flow conditions. Nowadays, existing traffic signal control systems in the field have different levels of coordination. The development of optimal signal control strategies that are network-wide coordinated and real-time applicable remains a challenge.

The field of urban traffic control has been studied and developed in a variety of ways during the past decades. A review of the literature related to road traffic control of the last century is given in [1]. In recent years, model predictive control (MPC) approaches have become more and more popular in road traffic control related research. MPC approaches for traffic systems predict the evolution of traffic dynamics and calculate the optimal control actions for the time period in which the relevant traffic dynamics occurs. This feature enables the controller to take advantage of potentially larger future gains at a current (smaller) cost, so as to avoid myopic control actions. MPC approaches that are based on the store-and-forward model for traffic flow optimization in saturated conditions are developed in [2] and [3]. Since the travel time on the roads between intersections is ignored, these approaches are less effective for under-saturated conditions. In [4] van den Berg *et al.* developed a non-linear MPC approach that is based on a detailed traffic flow model to optimize the network throughput. The complexity of the prediction model results in high computation time of the MPC problem. In [5] Lin *et al.* proposed a non-linear MPC and reformulated it into a mixed integer linear programming (MILP) problem that can be efficiently solved. In order to reduce computational complexity, this model assumes constant delay, which leads to the model inaccuracies in under-saturated traffic. Decentralized MPC strategies have been developed for urban traffic signal control in [6] and [7]. Even though decentralized MPC approaches increase the computation speed, they may result in sub-optimal control performances [8]. Recently, the macroscopic fundamental diagram (MFD) has been exploited as a basis for the derivation of urban signal control approaches [9]–[13]. Even though the MFD provides an efficient tool for the development of traffic control strategies for urban traffic networks, its accuracy in expressing aggregated dynamics of urban traffic networks, especially in case the network is characterized by a high density heterogeneity, still needs to be validated. Due to the complexity of urban traffic system, the development of MPC approaches of traffic signal control has to make a trade-off between model accuracy and computation time.

In the aforementioned MPC approaches, fixed turn fractions at intersections are assumed in order to simplify the prediction

Manuscript received November 20, 2017; revised June 29, 2018 and October 10, 2018; accepted October 14, 2018. The Associate Editor for this paper was B. Seibold. *(Corresponding author: Yu Han.)*

Y. Han is with Didichuxing LLC, Beijing 100193, China (e-mail: hanyudreamhunter@gmail.com).

A. Hegyi, Y. Yuan, and S. Hoogendoorn are with the Department of Transport & Planning, TU Delft, 2628CN Delft, The Netherlands (e-mail: a.hegyi@tudelft.nl; y.yuan@tudelft.nl; s.p.hoogendoorn@tudelft.nl).

C. Roncoli is with the Department of Built Environment, Aalto University, FI-00076 Espoo, Finland (e-mail: claudio.roncoli@aalto.fi).

Color versions of one or more of the figures in this paper are available online at http://ieeexplore.ieee.org.

Digital Object Identifier 10.1109/TITS.2018.2877259

1524-9050 © 2018 IEEE. Personal use is permitted, but republication/redistribution requires IEEE permission.
See http://www.ieee.org/publications_standards/publications/rights/index.html for more information.

This article has been accepted for inclusion in a future issue of this journal. Content is final as presented, with the exception of pagination.

models. As a matter of fact, there is a clear linkage between intersection control algorithms and route choice control [14]. Traffic route choice behavior is an important factor that influences the arriving flows at intersections. Thus, coordinating route choice control and intersection control will further improve traffic operation efficiency. However, the combination of route choice control and intersection control increases the complexity of the model, thus results in complicated optimization problems that cannot be solved efficiently [15]. Therefore, many studies regarding the optimization of traffic signals and route choice use heuristic approaches to solve the problem, which do not always lead to optimal results [16], [17]. The linear quadratic model predictive control (LQMPC) approach presented in [18] is a successful application to efficiently optimize turn fractions and traffic signals for single destination networks. However, due to the fact that the LQMPC has a discrete linear prediction model, traffic state in each discrete segment of the traffic network is aggregated and route choice behavior of traffic in each OD (Origin-Destination) pair is not considered. The controller pushes out traffic flow as much as possible, regardless of traffic desired origin and destination relations. Thus, the LQMPC approach may be ineffective when applied to multi-destination traffic networks, because the traffic may end up at wrong destinations.

In this paper, the problem that the existing LQMPC cannot preserve traffic OD relations is tackled by a heuristic method. We present two models: (1) a non-linear route-specific model which keeps track of traffic dynamics for each OD pair, and (2) a linear model that aggregates all route traffic states, which can be embedded into the LQMPC framework. For each OD pair, we define a set of links as the crucial links (c-links), which are links that traffic from the OD pair has to pass to reach the destination. Before each optimization run, the route-specific model predicts the route flow of every c-link based on a non-optimizing control strategy. In this paper, the non-optimizing control strategy we use is the integration of a simple routing strategy, which guides traffic flows at the origins to the route that has the shortest instantaneous travel time, and a simplified back-pressure algorithm for intersection signal timing plans [19]. In principle, any other routing and signal control approach could be used as the non-optimizing control strategy. In the optimization, we set constraints to the flows of c-links and the flows of the links towards destinations, to narrow the solution space and exclude unrealistic solutions that would lead to flows that are inconsistent with the OD relations. The optimal solution is evaluated by the route-specific model after each optimization run and compared with the non-optimizing control strategy. The control signals that leads to a better performance will be implemented. The evaluation process guarantees that the designed control approach never performs worse than the non-optimizing approach. The presented control approach is tested in a synthetic traffic network with multiple bottlenecks. It shows that the LQMPC achieves a total time spent close to the system optimal, while the computation time remains tractable.

The remaining of the paper is organized as follows. Section II presents the route-specific traffic flow model. Section III and Section IV present the existing LQMPC approach and the extended LQMPC approach respectively. Section V presents the design and testing results of a synthetic case. A summary and the discussion of future work conclude the paper in Section VI.

Fig. 1. The depiction of cells and links. Red arrows represent links, and black dashed lines represent the boundaries between cells. Origin cells have no incoming link and destination cells have no outgoing link. Normal cells are connected by one incoming link and one outgoing link.

II. Route-Specific Network Model

In this section, we present a route-specific macroscopic model. The traffic flow model is based on a discrete model, where the time is divided into discrete time steps and the roadway is divided into discrete cells. The definition of model variables are presented as follows.

A. Definition of Model Variables

Our representation of traffic networks is based on the queuing model developed in [18]. The model presented in this paper extends that model in two aspects. First, the previous model is a queuing model, which is not able to reproduce the propagation of congestion waves. In our model, we adopt the same logic as in the cell transmission model (CTM) to decide the boundary flows between cells, so as to capture the propagation of shock waves [20]–[22]. Second, routes are specified in each cell, to keep track of the traffic dynamics in each OD pair. The network elements and variables of the model are introduced as follows.

1) Cells and Links: In our model, roadway networks are divided into discrete cells and links. Cells are categorized into different types which include origin cells, destination cells, normal cells, merging cells, diverging cells, and intersection cells. The depiction of each type of cells can be found in Fig. 1 and Fig. 2. Vehicles flowing out of a cell move to downstream cells through pre-defined links. Links do not represent physical roadways, but an abstraction of the boundary that connects two consecutive cells.

Assume that time evolves in discrete steps, $t = 1, 2, 3, \ldots$, and traffic state of cell i is represented by the number of vehicles in a discrete time step t, which is denoted as $x_i(t)$. A link always connects two cells: we define the cell upstream of link j by Γ_j^{-1}, and the cell downstream of link j by Γ_j. The number of vehicles moving from one cell to another in a time step is defined as the traffic flow of a link, denoted by $f_j(t)$.

2) Routes: There may be multiple routes in a network, and each route connects one origin and one destination. In our model, routes are specified in each cell, and the number of vehicles following route r in cell i is denoted as $x_i^r(t)$. Accordingly, the traffic flow on a route of a link is denoted as $f_j^r(t)$. The traffic state of a cell and a link are the aggregations of the number of vehicles of every route in the cell and the

This article has been accepted for inclusion in a future issue of this journal. Content is final as presented, with the exception of pagination.

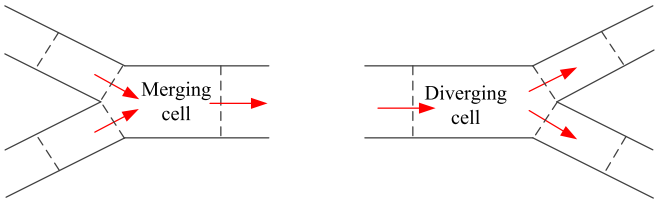

Fig. 2. The depiction of merging and diverging cells. Red arrows represent links. The incoming links of merging cells are called merging links and the outgoing links of diverging cells are called diverging links.

link:

$$x_i(t) = \sum_{\forall r} x_i^r(t), \tag{1}$$

$$f_j(t) = \sum_{\forall r} f_j^r(t). \tag{2}$$

3) Merge and Diverge: The cells that have one outgoing link and multiple incoming links are called merging cells, as shown in the left picture of Fig. 2. The cells that have one incoming link and multiple outgoing links are called diverging cells, as shown in the right picture of Fig. 2. We define the outgoing links of a diverging cell as diverging links, and the incoming links of a merging cell as merging links. The proportion of the flow of a diverging link j to the total flow that originate from the same diverging cell i is called turn fraction, which is denoted as $\theta_i^j(t)$. Traffic at a diverging cell may change their original routes based on the obtained information of road traffic conditions or the instructions received from the traffic control center. Thus, the variables $\theta_i^j(t)$ can be controlled by route guidance measures.

4) Intersections: In the following, we introduce the modeling of intersection flows. We define the cells directly upstream of the intersection conflict area as intersection cells. The outgoing links of intersection cells are defined as intersection links. We assume that flows of intersection links are always controlled by traffic lights. To avoid conflicting flows at an intersection, the green time of a cycle is divided into different phases such that conflicting flows do not get green at the same time. Assume that T_c represents the time duration of a cycle, then the green time duration of phase p at intersection s is $T_c \cdot u_s^p$, where u_s^p represents the green time fraction. At an intersection, the sum of the time fraction of each phase needs to satisfy the traffic light cycle constraint,

$$\sum^{p} u_s^p \le 1. \tag{3}$$

The set of link indices that get green at phase p is denoted as W_s^p. An intersection link may get green in different phases of a cycle, and the intersection link flow need to satisfy the green time fraction constraints,

$$f_j(t) \le \sum^{p} u_s^p(t) \cdot Q_j, \quad i \in C_I, \ \ j \in W_s^p, \ \ \Gamma_j^{-1} = i \tag{4}$$

where C_I is the set of intersection cell indices. Q_j [veh/h] is the saturation flow of intersection link j.

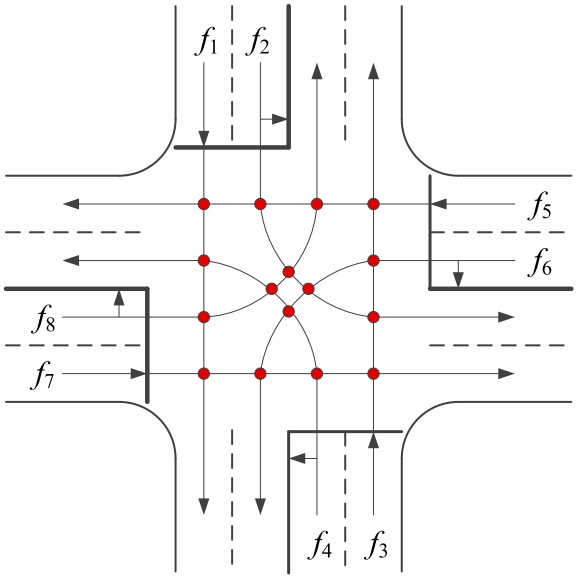

Fig. 3. An example intersection to explain the model variables. The figure is taken from [23]. $f_1, f_2, \ldots, f_8$ are the flows of intersection links. Red dots in the figure represent conflicting points of flows. The intersection is indexed as intersection 1. For simplicity, we assume that there are four phases in a cycle, and $W_1^1 = \{1, 3\}$, $W_1^2 = \{2, 4\}$, $W_1^3 = \{5, 7\}$, $W_1^4 = \{6, 8\}$. Note that there can be more phases in a cycle as long as the movements in each cycle do not conflict. u_1^1, u_1^2, u_1^3 and u_1^4 are the green time fraction of each phase so the traffic light cycle constraint is: $u_1^1+u_1^2+u_1^3+u_1^4 \le 1$. Green time fraction constraints are: $f_1 \le u_1^1 \cdot Q_1$, $f_2 \le u_2^2 \cdot Q_2$, $f_3 \le u_1^1 \cdot Q_3$, $f_4 \le u_1^2 \cdot Q_4$, $f_5 \le u_1^3 \cdot Q_5$, $f_6 \le u_1^4 \cdot Q_6$, $f_7 \le u_1^3 \cdot Q_7$, $f_8 \le u_1^4 \cdot Q_8$.

B. Updating of Traffic States

The route-specific traffic state of each type of cells is updated as follows.

Origin cells:

$$x_o^r(t+1) = x_o^r(t) + \left(q_{o,d}(t) \cdot \alpha^r - f_j^r(t)\right) \cdot T, \quad r \in R^{o,d}, \quad \Gamma_j^{-1} = o. \tag{5}$$

where o is the index of the origin cell, and (o, d) are the indices of OD pairs. $R^{o,d}$ is the set of route indices in the OD pair and $q_{o,d}(t)$ represents the demand of the OD pair at time t. T is the duration of a discrete time step. α^r is the fraction of the demand that chooses route r, and it is determined by a simple logit model which is formulated as:

$$\alpha^r = \frac{e^{(-\sigma \cdot \mathrm{TF}^r)}}{\sum_r e^{(-\sigma \cdot \mathrm{TF}^r)}}, \quad r \in R^{o,d} \tag{6}$$

where, TF^r is the free flow travel time of route r. σ is a scaling parameter that describes how drivers react on a travel time difference between the alternatives. This simple logit model represents how traffic chooses their routes at the origins, when it does not have any information of the traffic situation in the network [24].

Destination cells:

$$x_d^r(t+1) = x_d^r(t) + f_j^r(t), \quad \forall d \in C_D, \ \Gamma_j = d \tag{7}$$

where d is the index of destination cells and C_D is set of destination cell indices.

This article has been accepted for inclusion in a future issue of this journal. Content is final as presented, with the exception of pagination.

Normal cells and intersection cells:

$$x_i^r(t+1) = x_i^r(t) + f_j^r(t) - f_h^r(t), \quad \forall i \in C_N \cup C_I, \quad \Gamma_j = \Gamma_h^{-1} = i. \tag{8}$$

where C_N is the set of normal cell indices.

Merging cells:

$$x_i^r(t+1) = x_i^r(t) + \sum^{j} f_j^r(t) - f_h^r(t), \quad \forall i \in C_M, \ \Gamma_j = \Gamma_h^{-1} = i, \tag{9}$$

where C_M is the set of merging cells.

Diverging cells:

$$x_i^r(t+1) = x_i^r(t) + f_j^r(t) - \sum^{h} f_h^r(t), \quad \forall i \in C_V, \quad \Gamma_j = \Gamma_h^{-1} = i, \tag{10}$$

where C_V is the set of diverging cells.

The traffic flow updating procedure is presented as follows. Similar to the CTM, which uses a triangular fundamental diagram, we define a sending flow, $S_i(t)$, and a receiving flow, $R_i(t)$, for cell i. $S_i(t)$ and $R_i(t)$ are formulated as,

$$S_i(t) = \min\left(\frac{x_i(t)}{L_i} \cdot v_i, c_i\right),$$
$$R_i(t) = \min\left(\beta_i\left(\frac{x_i^J}{L_i} - \frac{x_i(t)}{L_i}\right), c_i\right), \tag{11}$$

where v_i and c_i are the free-flow speed and capacity of cell i. β_i is the congestion wave speed of cell i. x_i^J is the maximum number of vehicles in cell i. L_i is the length of cell i. For the links whose source cell and sink cell are normal cells, the flows are determined by the minimum between the sending flow and the receiving flow,

$$f_j(t) = \min(S_i(t), R_l(t)), \quad \forall i, l \in C_N, \ \Gamma_j^{-1} = i, \ \Gamma_j = l. \tag{12}$$

It is assumed that there is no route choice in normal cells. Thus the flow of every route is represented as,

$$f_j^r(t) = f_j(t) \cdot \frac{x_i^r(t)}{x_i(t)}, \quad \forall i \in C_N, \ \Gamma_j^{-1} = i \tag{13}$$

For a merging cell, the sending flow of the source cell is represented by the first equation of (11). The receiving flow is shared by multiple merging links. If the total sending flow is higher than the receiving flow, then the receiving flow needs to be distributed to each merging link. The sending flow of the source cell of a merging link is represented as,

$$S_i(t) = \min\left(\frac{x_i(t)}{L_i} \cdot v_i, c_i\right), \quad i \in C_M. \tag{14}$$

The merging flow updating procedure is presented as follows. Note that the receiving flow distribution process is the same as the first-order node model presented in [25].

1) The receiving flow is first distributed to the links, whose source cells have lower sending flow than the merging flow rate.
$$f_j(t) = S_i(t), \quad \text{if } S_i(t) \le R_l(t) \cdot \frac{c_i}{\sum_i c_i}, \quad l \in C_M \quad \Gamma_j^{-1} = i, \ \Gamma_j = l, \tag{15}$$
where, $R_l(t) \cdot \frac{c_i}{\sum_i c_i}$ is the merging flow rate of cell i. Once the receiving capacity is assigned to a link, the assigned flow is subtracted from the remaining receiving flow which is represented as $\tilde{R}_l(t)$.
2) Exclude the links which have been assigned, and calculate the remaining receiving flow. Update the merging flow rate for the remaining source cells and repeat the first step until no source cell has lower sending flow than the merging flow rate.
3) Distribute the remaining receiving flow to the remaining links, whose source cells have higher sending capacity than the merging flow rate:
$$f_j(t) = \tilde{R}_l(t) \cdot \frac{c_i}{\sum_i c_i} \tag{16}$$
4) The merging flow in each route is calculated by (13).

Traffic at a diverging cell may change its original route based on the obtained information of road traffic conditions or the instructions received from the traffic control center. In our model, we assume that if there is no control action, traffic continues traveling on its original routes. The turn fraction $\theta_i^j(t)$ of each diverging link is calculated as,

$$\theta_i^j(t) = \frac{\sum^{r} x_i^r(t)}{x_i(t)}, \quad r : j \in J^r \tag{17}$$

where J^r is the set of link indices in route r. Based on $\theta_i^j(t)$, the total flow of all the links, $l_1, l_2, \ldots, l_n$, that are leaving cell i, $F_i(t)$, is calculated as,

$$F_i(t) = \min\left(S_i(t), \frac{R_{l_1}(t)}{\theta_i^{l_1}(t)}, \frac{R_{l_2}(t)}{\theta_i^{l_2}(t)}, \ldots, \frac{R_{l_n}(t)}{\theta_i^{l_n}(t)}\right), \quad \forall i \in C_V. \tag{18}$$

The flow of each route is calculated as,

$$f_j^r(t) = F_i(t) \cdot \frac{x_i^r(t)}{x_i(t)} \quad \forall i \in C_V, \ \Gamma_j^{-1} = i \tag{19}$$

If route guidance control is applied at diverging cells, then $\theta_i^j(t)$ is the resulting turn fraction after control. The optimization problem is formulated as,

$$\min \sum^{r} x_{i,a}^r(t) \cdot \mathrm{TT}_i^r(t) \quad \forall i \in C_v$$
$$\text{subject to } \frac{\sum^{r} x_{i,a}^r(t)}{x_i(t)} = \theta_i^j(t), \quad r : j \in J^r$$
$$\sum^{r} x_{i,a}^r(t) = \sum^{r} x_{i,b}^r(t), \quad r : r \in R^{od} \tag{20}$$

where $\mathrm{TT}_i^r(t)$ is the instantaneous travel time of the part of route r, that starts from the diverging cell i. The first constraint in (20) ensures that the turn fraction of a diverging link j

This article has been accepted for inclusion in a future issue of this journal. Content is final as presented, with the exception of pagination.

equals to θ_i^j (the optimal value obtained from the controller) after re-routing, and the second constraint guarantees that the OD relations of the traffic in cell i unchanged. For diverging links, the total flow $F_i(t)$ is calculated according to (18) and the flow of each route is calculated based on (19) by changing $x_i^r(t)$ to $x_{i,a}^r(t)$. Note that the optimization problem (20) represents the autonomous process of the drivers' route choice, and it does not change the turn fractions.

As introduced in II-A, intersection flows are determined by the following equations,

$$f_j(t) = \min\left(S_i(t), R_l(t), \sum^p u_s^p(t) \cdot Q_j\right), \quad i \in C_I, \quad j \in W_s^p, \ \Gamma_j^{-1} = i, \ \Gamma_j = l, \quad (21)$$

and the flow in each route is calculated by (13).

III. The Classical LQMPC Approach

In [18] Le *et al.* presented an LQMPC approach based on a queuing model for optimal routing and intersection signal control of urban networks. Later, LQMPC approaches using extended discrete Lighthill-Whitham-Richards (LWR) models as prediction models have been presented for optimal ramp metering or variable speed limit control [26], [27]. In general, any model that has a linear formulation can be applied to the LQMPC framework. In this section, we present the general LQMPC framework using a discrete LWR model as the prediction model.

In the model, the states of cells and links are aggregated numbers of vehicles and aggregated flows, which are represented by $x_i(k)$ and $f_j(k)$, where k is the index of the discrete time step in the prediction. It is worth to note that the route-specific model presented in the previous section will be used to represent the reality, and the time index is t in that model. Usually the time step size of the prediction model is larger than the process model, because in the process model, detail traffic dynamics is usually needed but in the prediction model, a trade-off between the level of predicted details and the computation time has to be made. In this paper we use the same time step size for both the prediction model and the process model. Traffic states of each class of cells is predicted according to the following equations.

Origin cells:

$$x_o(k+1) = x_o(k) - f_j(k) + q_o(k), \quad \Gamma_j^{-1} = o$$
$$q_o(k) = \sum^o q_{o,d}(k) \quad (22)$$

Destination cells:

$$x_d(k+1) = x_d(k) + f_j(k), \quad \Gamma_j = d \quad (23)$$

Normal cells and intersection cells:

$$x_i(k+1) = x_i(k) + f_j(k) - f_h(k), \quad \forall i \in C_N, C_I, \quad \Gamma_j = \Gamma_h^{-1} = i. \quad (24)$$

Merging cells:

$$x_i(k+1) = x_i(k) + \sum^j f_j(k) - f_h(k), \quad \forall i \in C_M, \quad \Gamma_j = \Gamma_h^{-1} = i. \quad (25)$$

Diverging cells:

$$x_i(k+1) = x_i(k) + f_j^r(k) - \sum^h f_h(k), \quad \forall i \in C_V, \quad \Gamma_j = \Gamma_h^{-1} = i. \quad (26)$$

The flows must satisfy the following linear constraints,
Demand constraints:

$$f_j(k) \le \frac{x_i(k)}{L_i} \cdot v_i,$$
$$f_j(k) \le c_i, \quad \forall i \in C_O, C_N, C_M, C_I, \ \Gamma_j^{-1} = i \quad (27)$$
$$\sum^j f_j(k) \le \frac{x_i(k)}{L_i} \cdot v_i,$$
$$\sum^j f_j(k) \le c_i, \quad \forall i \in C_V, \ \Gamma_j^{-1} = i \quad (28)$$

Supply constraints:

$$f_j(k) \le \beta_i \cdot x_i^J\left(1 - \frac{x_i(k)}{x_i^J}\right),$$
$$f_j(k) \le c_i, \quad \forall i \in C_O, C_N, C_V, \ \Gamma_j = i \quad (29)$$
$$f_j(k) \le \beta_i \cdot x_i^J\left(1 - \frac{x_i(k)}{x_i^J}\right),$$
$$\sum^j f_j(k) \le c_i, \quad \forall i \in C_M, \ \Gamma_j = i. \quad (30)$$

Apart from the demand and supply constraints, intersection flows need to satisfy also the constraints of (3) and (4). The traffic dynamic can be represented by the following equation:

$$X(k+1) = X(k) + BF(k) + d(k) \quad (31)$$

where $X(k+1)$ is a vector of traffic states $x_i(k+1)$ of all the cells, excluding the destination cells. $F(k)$ is the vector of flows $f_j(k)$ of all the links. B is the matrix that contains topological information of the network. $d(k)$ is the demand vector, in which the non-zero values correspond to origin cells, and for the other cells the values are zero.

The objective of the LQMPC is to minimize the quadratic function of the number of vehicles in the network over the prediction horizon, $\hat{X}(k)$, in order to approximately minimize the total travel time. The prediction of $\hat{X}(k)$ over a horizon K_p is represented by the following equation:

$$\hat{X}(k) = AX(k) + B_1\hat{F}(k) + A_1\hat{d}(k), \quad (32)$$

This article has been accepted for inclusion in a future issue of this journal. Content is final as presented, with the exception of pagination.

where

$$\hat{X}(k) = \begin{bmatrix} X(k+1) \\ X(k+2) \\ \vdots \\ X(k+K_p) \end{bmatrix}, \quad A = \begin{bmatrix} I \\ I \\ \vdots \\ I \end{bmatrix},$$
$$\hat{F} = \begin{bmatrix} F(k) \\ F(k+1) \\ \vdots \\ F(k+K_p-1) \end{bmatrix}, \quad \hat{d} = \begin{bmatrix} d(k) \\ d(k+1) \\ \vdots \\ d(k+K_p-1) \end{bmatrix},$$
$$A_1 = \begin{bmatrix} I & 0 & \cdots & 0 \\ I & I & & \vdots \\ \vdots & & \ddots & \\ I & I & \cdots & I \end{bmatrix}, \quad B_1 = \begin{bmatrix} B & 0 & \cdots & 0 \\ B & B & & \vdots \\ \vdots & & \ddots & \\ B & B & \cdots & B \end{bmatrix}, \tag{33}$$

I is the identity matrix. The overall optimization problem is formulated as:

$$\begin{aligned} \min_{\hat{F}} \ & [AX(k) + B_1\hat{F}(k) + A_1\hat{d}(k)]'U \\ & [AX(k) + B_1\hat{F}(k) + A_1\hat{d}(k)] + G\hat{F} \\ \text{subject to equations (3)-(4), (22)-(30)} \\ & \hat{F}(k) \geq 0. \end{aligned} \tag{34}$$

where U is a matrix with all 1 elements. With this configuration the quadratic term aims to minimize the quadratic function of the number of vehicles in the network in the prediction horizon.

The quadratic term in the objective function is not exactly equivalent to the total travel time, nevertheless the previous work in [18] has demonstrated that the minimization of this objective function generally leads to good performance in reducing total travel time. G is a vector of cell lengths multiplied by a small negative value. The term $G\hat{F}$ aims to maximize the flows, so as to address the so-called holding back problem. Holding back may occur when the traffic state is congested and the traffic control measures cannot increase the outflows. In such a case, the quadratic term can lead to holding back of the traffic (because keeping traffic away from the congested parts can lead to a more homogeneous density distribution), while holding back is generally not favorable for travel time minimization. The term $G\hat{F}$ intends to discourage such holding back by slightly rewarding the forward movement of the traffic. The term was initially suggested in [28]. Note that this second term in (34) has a physical meaning, as it is proportional to the total travel distance (TTD). Thus, (34) may be perceived as a weighted combination of TTT minimization and TTD maximization. A more detailed explanation of this objective function can be found in [18]. The optimization problem can be solved by an appropriate solver (e.g., CPLEX). The outputs of the controller are optimal flows between cells.

Optimal control signals, i.e., green time fraction $u_s^p(k)$ and turn fraction $\theta_i^j(k)$, can be derived from the optimal flows by the following equations:

$$\theta_i^j(k) = \frac{f_j(k)}{\sum_{j:\Gamma_j^{-1}=i} f_j(k)},$$
$$u_s^p(k) = \frac{\sum_{j \in W_s^p} f_j(k)}{\sum_p \sum_{j \in W_s^p} f_j(k)}. \tag{35}$$

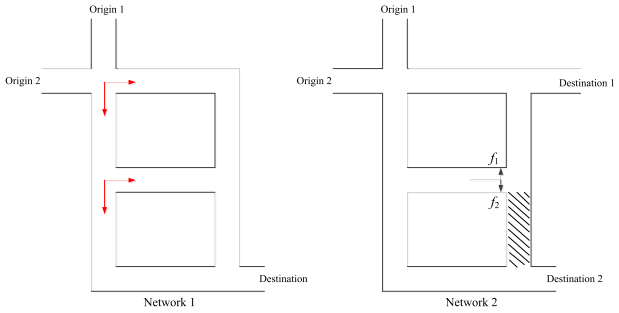

Fig. 4. Example networks to explain the usage of the LQMPC. Network 1 is a single destination network and network 2 is a multiple destination network. Red arrows in network 1 indicate the bifurcations, where traffic can make their route choices. Grey area in network 2 represents congestion. If the receiving flow of the gray area is 0, and the turn fraction of link 2 is higher than 0, then according to (18), both f_1 and f_2 are 0.

In [18], the LQMPC approach was applied to a single destination network for optimal vehicle routing, and the targeting network is shown as Network 1 in Fig. 4. In the network, route choices occur at bifurcations, which are shown as red arrows in Fig. 4. According to (34), traffic flows at bifurcations will be assigned to the optimal route, which leads to a minimum of system cost. However, when the LQMPC approach is applied to Network 2 in Fig. 4, the desired OD relations may not be preserved. Suppose that the whole network is in free flow state. Then the controller will assign as much traffic as possible to Destination 1 because it is closer to the origins so that the controller can achieve a lower cost by pushing out flows as quickly as possible. However, this is not realistic because traffic flows have their own intended destinations and the flow that is assigned to Destination 1 may intend to go to Destination 2. In other words, if we apply the optimal turn fraction θ_i^j obtained from (35) to the optimization problem in (20) for traffic assignment, there may be no feasible solution. In addition, traffic assignment errors in the LQMPC have a significant influence on the performance of signal control. For example, if the LQMPC assigns traffic flows from some OD pairs to a route that belongs to a different OD pair, then the intersection links in this route may get unnecessarily long green time because traffic in reality will not use these links. This may significantly decrease the efficiency of intersection control.

IV. An Extended LQMPC Approach

This section extends the method presented in the previous section to account for multiple destination networks. The reason why the previous LQMPC may not work for multi-destination networks is that the prediction model of the LQMPC does not have any information about the OD relations

This article has been accepted for inclusion in a future issue of this journal. Content is final as presented, with the exception of pagination.

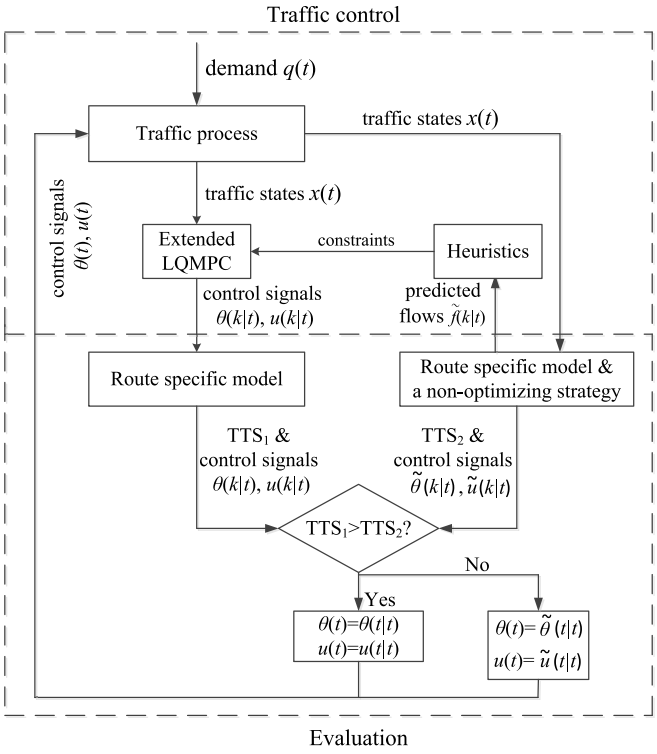

Fig. 5. The flowchart of the control approach. There are two blocks in this flowchart, where the upper block is the traffic control part and the lower block is the control performance evaluation part.

of traffic flows, thus traffic dynamics cannot be accurately predicted. The way we tackle this problem is to impose constraints (i.e., the lower or upper bounds of flows) to the LQMPC, to reduce the freedom of the controller in such a way that some unrealistic solutions, which may be optimal in the mathematical sense but not practically feasible, are excluded. The control approach is shown by a flowchart in Fig. 5. The extended LQMPC calculates the optimal flows based on real-time traffic states and predefined constraints to ensure the flow conservation at destinations. The constraints are set based on a heuristic method, in which the lower or upper bounds of flows are determined based on the OD relations of dynamic flows that are predicted by a forward simulation. The heuristic method intends to ensure the flow conservation at destinations, but cannot guarantee it. Thus, after each optimization run, the performance of the extended LQMPC is evaluated by the route-specific model. The performance of the extended LQMPC is compared with a non-optimizing control strategy, and the one that performs better is implemented into the process. This evaluation process ensures that the controller never performs worse than the non-optimizing approach.

The remaining of this section is set up as follows. Section IV-A presents the forward simulation method. Sections IV-B-IV-D introduce the heuristic approach to narrow the solution space and exclude unrealistic solutions. Section IV-E explains the evaluation process after each optimization run of the extended LQMPC.

A. Forward Simulation

Before each optimization run, we perform a forward simulation to predict dynamic flows that respect the given OD relations. The forward simulation runs based on the route-specific model using a non-optimizing control strategy, which is the integration of a simple routing strategy and a back-pressure algorithm for intersection timing plans. The routing strategy guides traffic flows to the routes that have the shortest instantaneous travel time. Traffic flows are assigned at the origins based on the instantaneous travel time of each route using equations (6) and (7), and it is assumed that there is no route choice for the traffic that is already in the network. A simplified back-pressure algorithm is used to determine the signal timing plans at intersections. For the original back-pressure algorithm, readers are referred to [19]. The integration of back-pressure traffic signal control and adaptive routing was explored in [29]. Note that any non-optimizing control strategy could be used in the forward simulation. In this paper, we use a simple routing strategy and a simplified back-pressure algorithm for convenience. The performance of the extended LQMPC may be related to the non-optimizing control strategy, because it serves as a lower bound of the performance of the proposed controller.

In the simplified back-pressure algorithm, there is a weight b_s^j associated with the link j at an intersection s. The weight is the difference in the number of vehicles between the source cell and the sink cell.

$$b_s^j(\tau) = x_i(\tau) - x_l(\tau), \quad j \in W_s^p, \ \Gamma_j^{-1} = i, \ \Gamma_j = l \tag{36}$$

The back-pressure algorithm determines the active phase p of intersection s at every time slot τ based on the back pressure B of phase p, $B_s^p(\tau)$. The back pressure $B_s^p(\tau)$ is the summation of link weights in that phase, which is formulated as,

$$B_s^p(\tau) = \sum^{j} b_s^j(\tau). \quad j \in W_s^p \tag{37}$$

The phase that has the maximum pressure is activated at τ. We assume that T_c is the time duration of a cycle and T_τ is the time duration of a slot time, and that T_c/T_τ is an integer. Then the green time fraction of phase p at intersection s is calculated as $\frac{n_s^p}{T_c/T_\tau}$, where n_s^p is the total number of activations of phase p in a cycle.

B. Minimum Flow Constraint on Each OD Pair

As introduced at the beginning of this section, the LQMPC may assign traffic flows to the routes that are not leading to their desired destinations, which is not realistic and may undermine the control performance. The reason is that the LQMPC has the freedom to assign flows to any connected links (if the receiving flows are high enough), which may result in unrealistic flow distributions, under the assumption that the destination are conserved, the flows cannot be realized. To this end, we restrict the freedom of the LQMPC by imposing hard constraints, to exclude unrealistic solutions that may deteriorate the control performance. To illustrate how the hard constraints are imposed, we first introduce the concept of crucial links (c-links).

For each OD pair a set of c-links is defined, among the links that are on the routes corresponding to the given OD pair. We first give an example where there is only one route for each

This article has been accepted for inclusion in a future issue of this journal. Content is final as presented, with the exception of pagination.

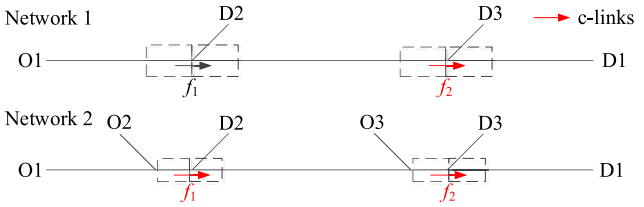

Fig. 6. An example to show the c-links (red arrows) of a specific OD pair that has a single route. Dashed rectangles represent cells and arrows represent links. In Network 1, link 2 is the c-link of OD pair O1-D1. In Network 2, links 1 and 2 are the c-links of O1-D1.

OD pair, shown as the networks in Fig. 6. In both networks, there are two bifurcations on the route that belong to the OD pair O1-D1, where the upstream one also directs to destination D2 and the downstream one also directs to destination D3. Traffic flows from O1 need to pass all the links in this route to reach the destination. Nevertheless, traffic flows may be guided to wrong destinations only at the bifurcations where the traffic from O1-D1 may be assigned to destinations D2 or D3. The same principle applies to other OD pairs of the network. In a route of an OD pair, if traffic flow of all diverging links that belong to the route comes from only one origin (e.g., the route of O1-D1 in Network 1), then only the most downstream link is a c-link because the flow that passes the most downstream diverging link must have passed all of the upstream diverging links. Therefore, only link 2 is the c-link in Network 1 whereas both links 1 and 2 are the c-links in network 2. The key of the extended LQMPC is to impose constraints to the flows of c-links, such that the predicted dynamic traffic flow satisfies the desired OD relations or alternatively has a small bias that does not have a significant influence on the control performance.

In Network 1, the c-link constraint of OD pair O1-D1 is formulated as,

$$f_2(k) \geq \tilde{f}_2^1(k), \quad k = t,\ t+1, \ldots, t+K_p-1. \tag{38}$$

where $\tilde{f}_2^1(k)$ is the flow of link 2 in route 1 (the route that belongs to O1-D1) that is predicted by the forward simulation. $\tilde{f}_2^1(k)$ is perceived as the lower bound of flow that needs to pass link 2 at time step k.

In Network 2, the c-link constraint of OD pair O1-D1 is formulated as,

$$\begin{aligned} &f_1(k) \geq \tilde{f}_1^1(k), \\ &f_2(k) \geq \tilde{f}_2^1(k), \quad k = t,\ t+1, \ldots, t+K_p-1. \end{aligned} \tag{39}$$

In Network 2, links 1 and 2 are also the c-links of OD pair O2-D1, thus links 1 and 2 are loaded with traffic flow from both O1-D1 and O2-D1. Under this circumstance, the c-link constraint is formulated as,

$$\begin{aligned} &f_1(k) \geq \tilde{f}_1^1(k) + \tilde{f}_1^2(k), \\ &f_2(k) \geq \tilde{f}_2^1(k) + \tilde{f}_2^2(k), \quad k = t,\ t+1, \ldots, t+K_p-1. \end{aligned} \tag{40}$$

where the route that belongs to O2-D1 is indexed by 2.

Now we extend the example to networks that have multiple routes in each OD pair, which are shown in Fig. 7. There are three routes in OD pair O1-D1, indexed as 1, 2, and 3 from top to bottom. Similar to the analysis of the single route example, link 1 (indicated by f_1) is the c-link of route 1 (i.e. traffic flow in O1-D1 that choose route 1 cannot reach the destination without passing link 1). Note that link 1 is a diverging link and other diverging links that originate from the same source cell may go to destination 3 or 4. Similarly, links 2 and 3 are the c-links of routes 2 and 3, thus links 1, 2, and 3 are the c-links of this OD pair. The c-link constraint of OD pair O1-D1 is formulated as,

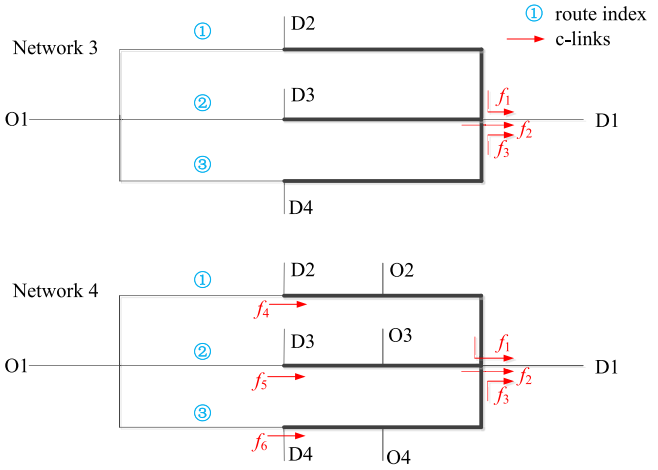

Fig. 7. An example to show the c-links of an OD pair that has multiple routes. Bold lines represent the roadways with two directions. In Network 3, links 1, 2, and 3 are the c-link of OD pair O1-D1. In Network 4, links 1, 2, 3, 4, 5, and 6 are the c-links of OD pair O1-D2.

$$\begin{aligned} f_1(k) + f_2(k) + f_3(k) \geq \tilde{f}_1^1(k) + \tilde{f}_2^2(k) + \tilde{f}_3^3(k), \\ k = t, t+1, \ldots, t+K_p-1. \end{aligned} \tag{41}$$

where the right-hand side of the inequality represents the lower bound of flow that needs to pass the c-links of O1-D1. Note that such constraint does not restrict the route choice freedom of traffic flow. In Network 4, traffic flow from different origins is added to the network. Similar to the analysis of the single route example, links 1 and 4 are the c-links of route 1, links 2 and 5 are the c-links of route 2, and links 3 and 6 are the c-links of route 3. We use $J^r_{\mathrm{C}(o,d)}$ to represent the set of c-links of route r in OD pair (o, d). For readability, we use J to represent $J_{\mathrm{C}(o,d)}$ in equations (43) and (44). In this example, $J^1_{\mathrm{C}(o,d)} = \{1, 4\}$, $J^2_{\mathrm{C}(o,d)} = \{2, 5\}$, and $J^3_{\mathrm{C}(o,d)} = \{3, 6\}$. The c-link constraint of O1-D1 is formulated as,

$$\begin{cases} f_1(k) + f_2(k) + f_3(k) \geq \tilde{f}_1^1(k) + \tilde{f}_2^2(k) + \tilde{f}_3^3(k) \\ f_1(k) + f_2(k) + f_6(k) \geq \tilde{f}_1^1(k) + \tilde{f}_2^2(k) + \tilde{f}_6^3(k) \\ \vdots \\ f_4(k) + f_5(k) + f_6(k) \geq \tilde{f}_4^1(k) + \tilde{f}_5^2(k) + \tilde{f}_6^3(k). \end{cases} \tag{42}$$

In each inequality, the left hand side contains one of the c-links from each route. The c-links of a route are indexed as $\varkappa^r$, and $\varkappa^r = 1, 2, \ldots, \kappa^r$. The general formulation of (38-39) and (41-42) is,

$$\begin{aligned} \sum^{r} f_{J^r(\varkappa^r)}(k) \geq \sum^{r} f^r_{J^r(\varkappa^r)}(k), \\ \forall r \in R^{o,d}, \quad \forall \varkappa^r = 1, 2, \ldots, \kappa^r. \end{aligned} \tag{43}$$

This article has been accepted for inclusion in a future issue of this journal. Content is final as presented, with the exception of pagination.

If link j is the c-link of multiple OD pairs, i.e., $\exists\, r' \in R^{o',d'}$, $(o',d') \neq (o,d)$: $j = J^{r}_{\mathrm{C}(o,d)}(\varkappa^{r}) = J^{r'}_{\mathrm{C}(o',d')}(\varkappa^{r'})$, then the right hand side of each OD pair's inequalities that contains the route flow of link j need to be integrated, like the example shown in equation (40). The general formulation of (40) is,

$$\sum^{r} f_{J^{r}(\varkappa^{r})}(k) \geq \sum^{o,d}\sum^{r} f^{r}_{J^{r}(\varkappa^{r})}(k), \quad \forall r \in R^{o,d}, \quad \forall \varkappa^{r} = 1, 2, \ldots, \kappa^{r}. \tag{44}$$

To summarize, we elaborate several features of c-links: (i) C-links are the diverging links that do not direct traffic to the same destination. (ii) If the most downstream diverging link of a route has a destination choice, then it is a c-link. (iii) If traffic from other origins joins the links that are located between two consecutive diverging links, then the upstream diverging link is a c-link. We present a generic algorithm to search for the c-links of each route. $J^{r}_{\mathrm{V}(o,d)}$ is the set of diverging links in route r. The diverging links are indexed as v^{r}, and the diverging links in route r are represented as $J^{r,v^{r}}_{\mathrm{V}(o,d)}$. $v^{r} = 1, 2, \ldots, \vartheta^{r}$, numbered from downstream to upstream.

$\varkappa^{r} = 1;$
$v^{r} = 1;$
$\forall j'\colon \Gamma^{-1}_{j'} = \Gamma^{-1}_{J^{r,v^{r}}_{\mathrm{V}(o,d)}}$, *if* $\exists\, r, \exists\, d'\colon j' \in J^{r}, r \in R^{o,d'}, d' \neq d$
  $J^{r,\varkappa^{r}}_{\mathrm{C}(o,d)} = J^{r,v^{r}}_{\mathrm{V}(o,d)};$
  $v^{r} = v^{r} + 1;$
end
for $v^{r} = 1\colon \vartheta^{r}$
  $\forall o' \neq o$, *if* $\exists\, r \in R^{o,d'} : J^{r,v^{r}}_{\mathrm{V}(o,d)} \in J^{r}$, $J^{r,v^{r}+1}_{\mathrm{V}(o,d)} \notin J^{r}$
    if $v^{r} + 1 \leq \vartheta^{r}$
      $J^{r,\varkappa^{r}+1}_{\mathrm{C}(o,d)} = J^{r,v^{r}+1}_{\mathrm{V}(o,d)};$
      $v^{r} = v^{r} + 1;$
    end
  end
end

C. Reproducing Spillback

The c-link constraint narrows the solution space of the LQMPC such that the OD relations are better preserved. However, the LQMPC with the c-link constraint cannot reproduce spillback. Spillback is a phenomenon that the congestion of a downstream link affects the possible outflow volume of an upstream link. The route-specific model presented in Section II is able to reproduce spillback. For example, if the grey area in network 2 of Fig. 4 is fully blocked (the receiving flow is 0), and the turn fraction of link 2 is higher than 0, then according to (18-19), the total flow of f_1 and f_2 is 0. The classical LQMPC approach introduced in the previous section is not able to reproduce the spillback phenomenon because the LQMPC always limits the turn fraction of a link to zero (or one, or small or large enough) if one of the receiving cell is congested, in such a way that the outflow to other links is still maximal. However, such kind of traffic assignment is not always realistic. If all of the traffic flows that intend to pass the congested link can reach their desired destinations by changing routes to the uncongested links, then it is realistic for the LQMPC to limit the turn fractions of the congested links to 0.

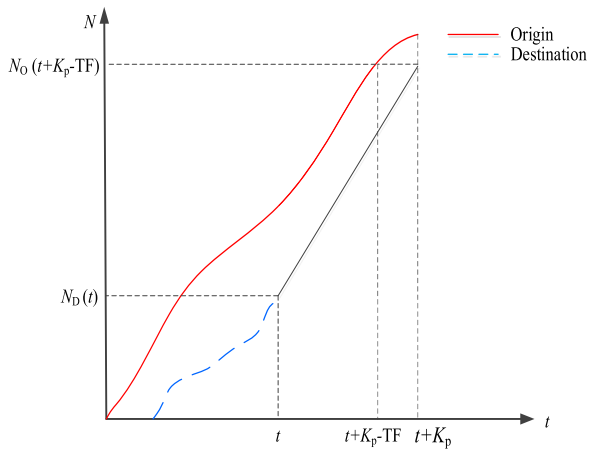

Fig. 8. The cumulative curves, representing the number of vehicles, at the origin and the destination of an OD pair. The red line is the cumulative curve at the origin $N^{o,d}_{\mathrm{O}}(t)$ and the dashed blue line is the cumulative curve at the destination $N^{o,d}_{\mathrm{D}}(t)$. Assuming that the controller runs at t and that $\mathrm{TF}_{o,d}$ is the free flow travel time for the considered OD pair, the difference between $N^{o,d}_{\mathrm{O}}(t + K_{\mathrm{p}} - \mathrm{TF}_{o,d})$ and $N^{o,d}_{\mathrm{D}}(t)$ is the maximum number of vehicles that can reach destination d from origin o during $(t,\ t + K_{\mathrm{p}})$. Thus, the maximum number of vehicles that may reach destination d is $\sum^{o}\left(N^{o,d}_{\mathrm{O}}(t + K_p - \mathrm{TF}_{o,d}) - N^{o,d}_{\mathrm{D}}(t)\right)$.

Nevertheless, if some traffic flows cannot reach their desired destinations by changing their routes, then it is not realistic to avoid spillback by forcing traffic to change their routes. If the LQMPC still limits the turn fractions of the congested links to 0, there will be a discrepancy between traffic dynamics that predicted by the LQMPC and real traffic dynamics, which may have a significant influence on the control performance.

In the classical LQMPC, the supply constraint (30) is imposed to each individual diverging link. To reproduce spillback, the supply constraint should be imposed to the total flow of all diverging link that originate from one diverging cell, as explained in equation (18). To this end, we define a minimum turn fraction of a diverging link, $\theta^{i,j}_{\min}(k)$, which indicates the proportion of traffic flow that cannot reach their desired destination without passing link j. Since the route-specific model keeps track of the OD relations of traffic flows, $\theta^{i,j}_{\min}(k)$ can be easily obtained from the forward simulation. According to (18), the following constraint is added to the LQMPC to reproduce spillback.

$$\sum_{v=1}^{n} f_{l_v}(k) \leq \min\left(\frac{R_{l_1}(t)}{\theta^{i,l_1}_{\min}(t)}, \frac{R_{l_2}(t)}{\theta^{i,l_2}_{\min}(t)}, \ldots, \frac{R_{l_n}(t)}{\theta^{i,l_n}_{\min}(t)}\right), \quad \forall i \in C_V, \quad k = t, t+1, \ldots, t+K_p-1. \tag{45}$$

D. Destination Constraint

The extended LQMPC always has a tendency to assign traffic flows to attractive destinations where traffic can leave the network faster, even if the c-link constraint is imposed. To avoid that the traffic flows assigned to attractive destinations are higher than the maximum flows, we add the so-called destination constraint to balance the flows arriving at each destination.

This article has been accepted for inclusion in a future issue of this journal. Content is final as presented, with the exception of pagination.

The destination constraint is set based on the maximum possible arriving flow of each destination. As shown in Fig. 8, the red line represents the cumulative curve at the origin of an OD pair, and the dashed blue line represents the cumulative curve at the destination of this OD pair. Suppose that the controller runs at time t, then the maximum possible number of vehicles that can arrive at the destination within the prediction horizon K_p is $\sum^{o}\left(N_\mathrm{O}^{o,d}(t+K_\mathrm{p}-\mathrm{TF}_{o,d})-N_\mathrm{D}^{o,d}(t)\right)$, where $\mathrm{TF}_{o,d}$ is the free flow travel time of the OD pair. $N_\mathrm{O}^{o,d}(t)$ and $N_\mathrm{D}^{o,d}(t)$ are the cumulative number of vehicles at the origin and the destination, respectively. We set the following constraint to the extended LQMPC, to ensure the flow that arrives at each destination proportional to the maximum possible number of vehicles that can arrive to the destination within the prediction horizon.

$$\frac{\sum_{k=t}^{t+K_\mathrm{p}-1} f_j(k)}{\sum_{k=t}^{t+K_\mathrm{p}-1} f_{j'}(k)} = \frac{\sum^{o}\left(N_\mathrm{O}^{o,d'}(t+K_p-\mathrm{TF}_{o,d'})-N_\mathrm{D}^{o,d'}(t)\right)}{\sum^{o}\left(N_\mathrm{O}^{o,d'}(t+K_\mathrm{p}-\mathrm{TF}_{o,d'})-N_\mathrm{D}^{o,d'}(t)\right)},$$
$$\forall d, d' \in C_D, \quad \Gamma_j = d, \ \Gamma_{j'} = d'. \quad (46)$$

The destination constraint balances the number of vehicles that arrive at each destination, to avoid that redundant traffic flow is assigned to attractive destinations. For example, if a bottleneck is activated, which may block the flow that will arrive at a (unattractive) destination, then the LQMPC without the destination constraint will try to push the flow to other destinations to maximize throughput. Under such circumstance, the LQMPC with the destination constraint tries to resolve the congestion first, because if the flow that arrives at the unattractive destination is low, the flows that arrives at any other destinations will be low as well.

E. Evaluation Step of the Extended LQMPC

We assume that the route-specific model introduced in Section II is accurate enough to represent reality and we employ the route-specific model in a model predictive control framework to optimize the network performance (e.g., minimize the total time spent). The optimization problem is formulated as,

$$\min \sum_{r}\sum_{\forall i \notin C_D}^{i}\sum_{k=t}^{t+K_p-1} x_i^r(k)\cdot T$$
subject to (1)-(19)
$$f_j(k) \geq 0, \quad \forall k = t, t+1, \ldots, t+K_p-1. \quad (47)$$

where C_D is the set of destination cells. The above optimization problem is non-linear because the traffic dynamics represented by the route-specific model is non-linear. The original MPC can be perceived as a simplification of the non-linear optimization problem. However, the solution space of the original LQMPC is larger than the non-linear optimization, because the original LQMPC has the freedom to assign vehicles to any links even if they do not lead to the desired destination. A conceptual depiction of the solution spaces of the different formulations is shown in Fig. 9, where the solution boundary of the non-linear optimization is shown as the blue line. If the optimal solution of the original LQMPC lies in the boundary of the solution space (the red line), then it has a large bias towards the optimal solution of the non-linear optimization, which may have a significant influence on the control performance.

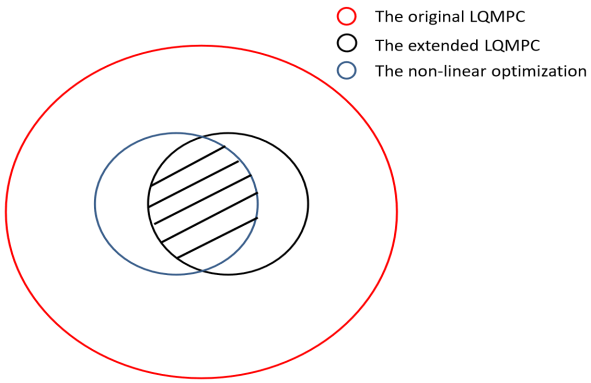

Fig. 9. A conceptual explanation about the boundaries of the solution spaces of the original LQMPC (the red line), the extended LQMPC (the black line), and the non-linear optimization (the blue line).

The c-link constraint and the destination constraint introduced in the previous sections narrow the solution space of the LQMPC to exclude unrealistic solutions. In other words, the inclusion of the constraints reduces the distance of the solution space boundary between the extended LQMPC and the non-linear optimization. Therefore, even if the optimal solution of the extended LQMPC lies in the boundary of the solution space (shown as the dashed blue line in Fig. 9), it will have less influence to the control performance.

Note that the constraints cannot guarantee the solution space of the extended LQMPC to be exactly the same as the non-linear optimization. To avoid extremely bad performance of the extended LQMPC, we evaluate the performance of the extended LQMPC at the end of each optimization run. As shown in Fig. 5, the optimal control signals obtained from the extended LQMPC are implemented into the route-specific model and compared with the ones of the non-optimizing control strategy. If the performance of the non-optimizing strategy is better than the extended LQMPC, then the non-optimizing actions are implemented for real-time traffic control.

V. Case Study

We test the performance of the presented control approach in a synthetic network, in Fig. 10, which contains 7 OD pairs and two signalized intersections, whose movements are shown in Fig. 11. The bold line that connects A and B represents a two-lane urban expressway, while other lines represent one-lane urban arterial roads. This network contains two potential bottlenecks, which are denoted as 'BN1' and 'BN2' in Fig. 10. BN1 represents an accident area, and the capacity of this area reduces to half of the free flow capacity when it is activated, whereas BN2 represents the blockade of the downstream boundary, and the capacity of this area reduces

This article has been accepted for inclusion in a future issue of this journal. Content is final as presented, with the exception of pagination.

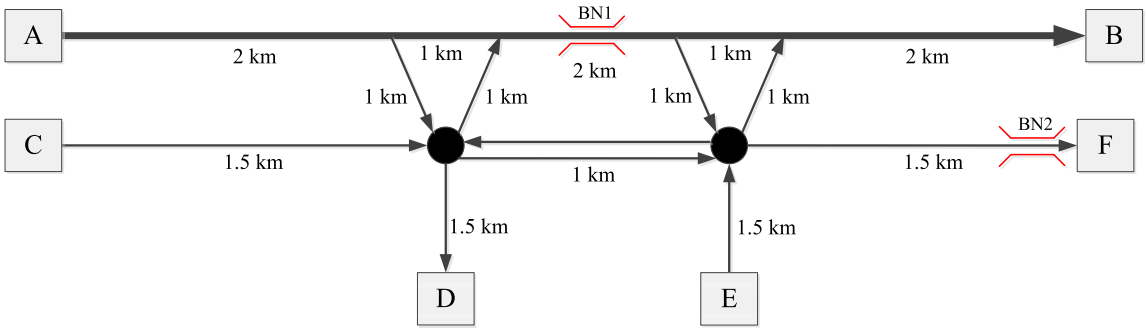

Fig. 10. Sketch of the synthetic network. The bold line indicates freeway and other lines indicate urban arterials. 'BN1' and 'BN2' represent bottlenecks. The circles represent signalized intersections.

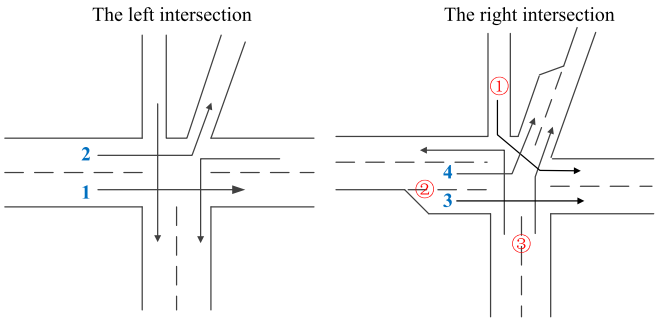

Fig. 11. The depiction of the movements. Red circled numbers in the right intersection are the index of roadway sections at the upstream of the intersection. Blue numbers represent the index of some of the links.

TABLE I
THE DEMAND PATTERN OF THE SYNTHETIC CASE

OD pairs	AB	AD	AF	CB	CF	EB	ED
Demand veh/h	1500	150	500	1000	500	300	150

to one-third of the free flow capacity when it is activated. Finally, we employ the demand patterns shown in Tab. I. In all experiments presented in this paper, we assume that the OD flows are known; if this information is not available, one may employ an on-line OD estimation method [30].

The route-specific model is used as the process model to represent reality. The parameters of the process model are set up as follows. The free flow speed v and the cell length l are set to 120 (km/h) and 1 (km/cell) for the freeway, and 60 (km/h) and 0.5 (km/cell) for urban roads. The duration of one simulation step, T, is set to 30s, which satisfies the CFL condition. The capacity c is set to 2000 (veh/h/lane) for the freeway and 1800 (veh/h/lane) for urban roads. The saturation flow Q of intersection movements are set to 1800 (veh/h). The congestion wave speeds for all cells are set to -20 (km/h). The parameter σ, which is used to model traffic route choices at origins, is set to 0.05 (1/s).

Three control scenarios are tested in the synthetic case study.

1) Scenario 1 is the reference scenario which indicates that the solution is close to the system optimum. The route-specific model is used as both the prediction model and the process model. The prediction horizon K_p is set to 15 minutes and the control horizon K_c is set to 30 seconds. The non-linear optimization problem is solved by MATLAB implementation of the SQP algorithm (fmincon).
2) Scenario 2 applies the presented extended LQMPC. K_p and K_c are set to same values as in scenario 1. In the forward simulation, the slot time τ of the simplified back-pressure algorithm is set to 1 second. The optimization of LQMPC is solved by CPLEX from MATLAB toolbox.
3) Scenario 3 applies the non-optimizing control strategy. The slot time τ of the simplified back-pressure algorithm is set to 1 second. Traffic is routed at the origins according to (6) based on the instantaneous travel time.

We test the performance of the three control scenarios for a simulation period of an hour. It is assumed that 'BN1' is activated during the first half an hour and 'BN2' is activated during the second half an hour. During the first half an hour, due to the capacity reduction of the freeway, we expect that controllers assign less traffic flow that comes from origin C to the freeway, to avoid congestion occurs at the freeway bottleneck. During the second half an hour, the demand of destination F is higher than the maximum outflow, therefore, if the congestion propagates to the intersection and blocks link 3 (see Fig. 11), then the flow of link 4 is also blocked, which results in a reduction of the outflow at destination B. Thus, we expect that controllers prevent the blockade of the intersection for as long as possible.

In addition, to investigate how OD relations are preserved by the original LQMPC, we run the simulation of another scenario (scenario 4) where both the process model and the prediction model are the macroscopic model that does not keep track of flows in each route. In this scenario we do not use the destination preserving process model, becasue it is not straightforward to simulate infeasible solutions with the presented process model. The presented process model assign traffic flows to different routes through an optimization problem, i.e. equation (20). If a controller (e.g., the LQMPC) generates infeasible turn fractions, the traffic assignment in the presented process model will not have a feasible solution.

The Total Time Spent(TTS) of the four control scenarios are 322.5h, 324.7h, 544.8h, 126.2 h respectively. The outflows of destinations B, D, and F in every scenario are shown in Fig. 12 (a), (b), and (c). There is a significant difference between the

This article has been accepted for inclusion in a future issue of this journal. Content is final as presented, with the exception of pagination.

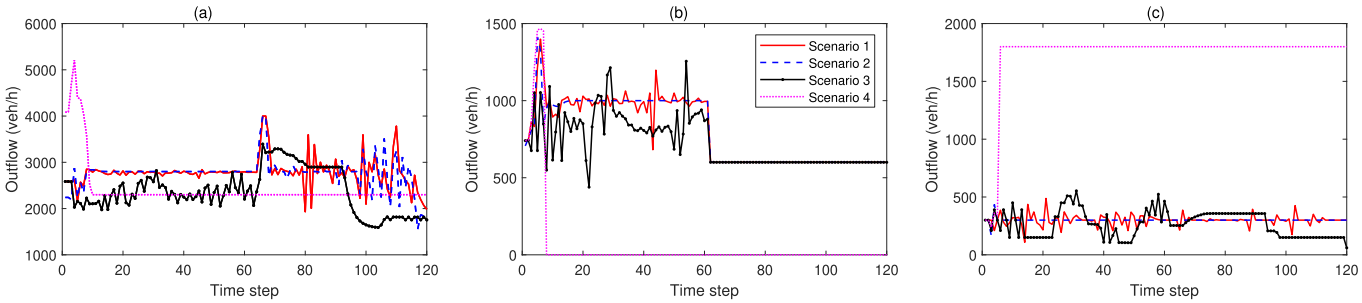

Fig. 12. Outflow of each destination in very scenario. (a), (b), and (c) are ouflows of destinations B, D, and F. Red, blue, black, and pink lines represent scenarios 1, 2, 3, and 4 respectively.

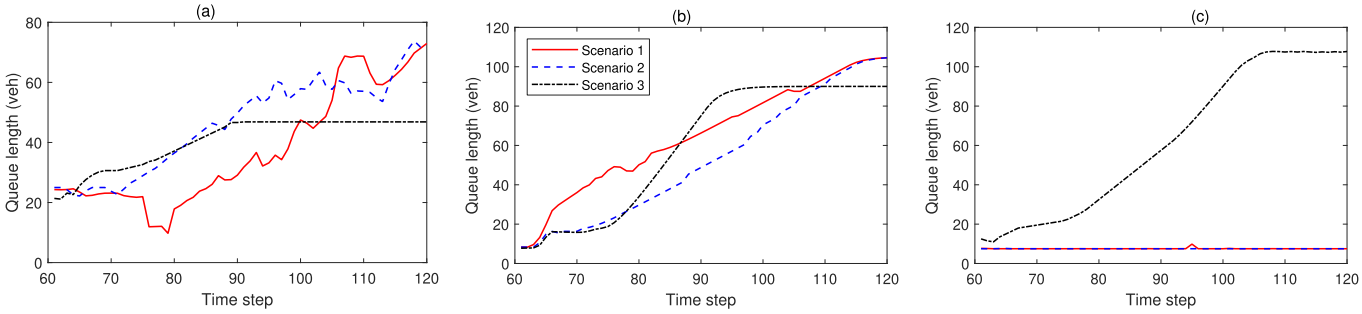

Fig. 13. Queue lengths of section 1, 2 and 3 in Fig. 11 in scenarios 1, 2, and 3. (a), (b), and (c) are queue lengths of destinations B, D, and F. Red, blue, and lines represent scenarios 1, 2, and 3 respectively.

outflows for each destination in scenario 4 with respect to other scenarios. The original LQMPC assigns more flows (around 2000 veh/h) from destination D and less flows (nearly 0) from destination F. This is because destination D is closer to the origins and the controller can achieve a lower cost by assigning a very high flow to destination D. However, this violates the conservation of destinations because the desired demand at destination D is, in fact, limited(300 veh/h). Therefore, even though the original LQMPC achieves a small TTS, it cannot be applied to reality because these results are based on incorrect OD relations.

The performances of scenarios 1, 2, and 3 are reflected by Fig. 12. At the first 60 steps (half an hour), the outflows in scenario 2 (the presented control approach) are generally higher than in scenario 3 (the non-optimizing control approach). This is attributed to the better operation of the route guidance. Due to the fact that the capacity at BN1 is only 2000 veh/h and traffic flows of OD pairs AB and AF (the total demand of which is 2000 veh/h) have to pass BN1, extra traffic flow that comes from origin C will trigger congestion on the freeway. As a consequence, the controller in scenario 2 assigns all of the flow from origin C to urban roads. As shown by the blue line in Fig. 14, in the first 60 steps the turn fraction of link 1 in Fig. 11 is 1, which means that the controller assigns all of the flow from origin A to urban roads to avoid triggering congestion on the freeway. On the other hand, the non-optimizing approach assigns traffic flows based on the instantaneous travel time, and the turn fraction shows oscillated behavior. Once the freeway has a lower instantaneous travel time, the controller assigns more flows to the freeway which results in travel time increasing and turn fraction decreasing, and vice versa. Consequently,

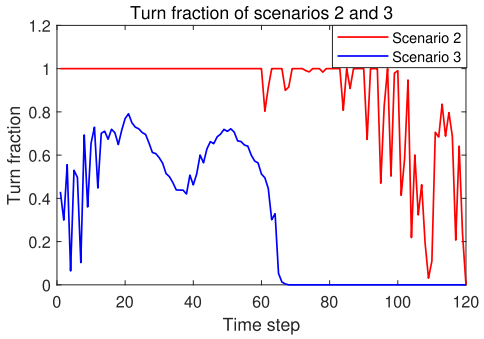

Fig. 14. Turn fraction of link 1 at the left intersection in Fig. 11. Red line represents scenario 2 and blue line represents scenario 3.

the outflow also shows an oscillating behavior and, when the turn fraction of link 1 is high, the outflow are also high because more traffic flow avoids being delayed in the congestion that occurs on the freeway. The presented control approach keeps high outflow for the first 60 steps, which is close to the system optimal controller.

In the second 60 steps, the capacity at BN1 recovers to 4000 (veh/h) and a new bottleneck, BN2, is activated. The total demand of destination F is 1000 (veh/h), which is higher than the maximum outflow of the bottleneck, 600 (veh/h). Thus, congestion occurs at destination F and propagates to the right intersection. If the road section at the upstream of destination F is fully blocked, the flows of both link 3 and 4 in Fig. 11 are 0, which will reduce the outflow of destination B. Thus, the controller needs to gate the flow at road section 3 to prevent the congestion spillbacks to the intersection. Controllers of scenario 1 (system optimal) and scenario 2

This article has been accepted for inclusion in a future issue of this journal. Content is final as presented, with the exception of pagination.

(the presented control approach) have similar control patterns. As shown by the dashed lines in Fig. 13 (b), a queue is accumulated at road section 2 from time step 60. The gating of road section 3 generates a queue, which, if it back-spilling to the freeway, the freeway mainstream flow will reduce and the outflow of destination B will decrease. Thus, the controller should balance the queue lengths of road sections 1 and 2 to avoid the reduction of the total outflow for as long as possible. At the end of the simulation, since both sections 1 and 2 are blocked and the controller cannot gain any benefit from gating, the outflow starts decreasing. For the non-optimizing control approach, as shown in Fig. 13, the controller balances of queue lengths of sections 1, 2, and 3 because of the feature of the back-pressure algorithm. However, gating at road section 3 but releasing the flows of road sections 1 and 2 prompts the blockade of the intersection. Thus, the outflow of destination B in scenario 3 starts decreasing before time step 90, which is much earlier than which in scenarios 1 and 2.

We employ for optimization and simulation a personal computer with an E5-1620 processor and 16 GB RAM. The computation time of the presented controller and the system optimal controller are 1.2 seconds per control step and 89 seconds per control step, respectively. In this case study, the presented controller achieves a performance that is close to the system optimal performance, while it keeps a tractable computation time. It is expected that employing a different, more advanced, numerical algorithm for computing the solution in the system optimal control case instead of the SQP algorithm, such as, for example, the ones used in [31], would improve the computational performance. On the other hand, any non-linear programming method presents some disadvantages with respect to LQMPC. In fact, LQMPC not only generates a globally optimal solution with less computational time, but it also guarantees convergence independently on any initial guess (which is necessary in the system optimal control case). In addition, even in case the system optimal control case converges in a reasonable time, the solution may be trapped in a local optimum, while any algorithm targeting at avoiding local optima (e.g., multi-start) would substantially increase computational time. Finally, an increase in size of the optimization problem (e.g., considering a bigger network or extending the prediction horizon) is expected to affect more consistently the computational time of the system optimal control case with respect to the proposed LQMPC, since the latter belongs to the category of QP problems, which has been proven being characterized by polynomial complexity [32]. The quantitative relation between the size of the optimization problem and the computation time of the extended LQMPC will be investigated in the future.

VI. Conclusions

In this paper, we presented an extended LQMPC approach for multi-destination networks. The previously proposed LQMPC approach is ineffective for multi-destination networks because the prediction model cannot preserve traffic OD relations. The optimal solution of the previous LQMPC may violate the flow conservation of destinations, which may significantly influence the control performance. To overcome this shortcoming, we introduced a heuristic method to narrow the solution space of the LQMPC by introducing additional constraints, so as to exclude unrealistic solutions. In principle, not all of the unrealistic solutions can be excluded by the constraints and it is still possible that the optimal solution does not conserve destinations. To this end, we evaluate the control performance at the end of each optimization run. The performance of the extended LQMPC is compared with a non-optimizing control approach, and the one that has a better performance is implemented to the process. This approach ensures that the presented control approach never has a worse performance than the non-optimizing approach.

The presented control approach is tested in a synthetic network that has multiple bottlenecks. When the bottleneck appears at the expressway, the controller effectively assigns traffic flows to the parallel arterial road, and when the bottleneck appears at an urban intersection, the controller effectively gates flow to maximize the intersection outflow. It is of particular significance that the computation time of the presented control approach is real-time tractable, which is essential for field applications. A future step is to test the presented approach by using microscopic simulation tools. It is also interesting to investigate how to reformulate the linear constraints of the extended LQMPC such that the optimization outperforms the non-optimizing approach in all cases.

References

[1] M. Papageorgiou, C. Diakaki, V. Dinopoulou, A. Kotsialos, and Y. Wang, "Review of road traffic control strategies," *Proc. IEEE*, vol. 91, no. 12, pp. 2043–2067, Dec. 2003.

[2] K. Aboudolas, M. Papageorgiou, and E. Kosmatopoulos, "Store-and-forward based methods for the signal control problem in large-scale congested urban road networks," *Transp. Res. C, Emerg. Technol.*, vol. 17, no. 2, pp. 163–174, Apr. 2009.

[3] K. Aboudolas, M. Papageorgiou, A. Kouvelas, and E. Kosmatopoulos, "A rolling-horizon quadratic-programming approach to the signal control problem in large-scale congested urban road networks," *Transp. Res. C, Emerg. Technol.*, vol. 18, no. 5, pp. 680–694, Oct. 2010.

[4] M. van den Berg, A. Hegyi, B. D. Schutter, and J. Hellendoorn, "Integrated traffic control for mixed urban and freeway networks: A model predictive control approach," *Eur. J. Transp. Infrastruct. Res.*, vol. 7, no. 3, pp. 223–250, Sep. 2007.

[5] S. Lin, B. De Schutter, Y. Xi, and H. Hellendoorn, "Fast model predictive control for urban road networks via MILP," *IEEE Trans. Intell. Transp. Syst.*, vol. 12, no. 3, pp. 846–856, Sep. 2011.

[6] E. Camponogara and L. B. De Oliveira, "Distributed optimization for model predictive control of linear-dynamic networks," *IEEE Trans. Syst., Man, Cybern. A, Syst., Humans*, vol. 39, no. 6, pp. 1331–1338, Jun. 2009.

[7] L. B. de Oliveira and E. Camponogara, "Multi-agent model predictive control of signaling split in urban traffic networks," *Transp. Res. C, Emerg. Technol.*, vol. 18, no. 1, pp. 120–139, Feb. 2010.

[8] J. R. D. Frejo and E. F. Camacho, "Global versus local MPC algorithms in freeway traffic control with ramp metering and variable speed limits," *IEEE Trans. Intell. Transp. Syst.*, vol. 13, no. 4, pp. 1556–1565, Dec. 2012.

[9] M. Keyvan-Ekbatani, A. Kouvelas, I. Papamichail, and M. Papageorgiou, "Exploiting the fundamental diagram of urban networks for feedback-based gating," *Transp. Res. B, Methodol.*, vol. 46, no. 10, pp. 1393–1403, Dec. 2012.

[10] J. Haddad, M. Ramezani, and N. Geroliminis, "Cooperative traffic control of a mixed network with two urban regions and a freeway," *Transp. Res. B, Methodol.*, vol. 54, no. 8, pp. 17–36, Aug. 2013.

[11] N. Geroliminis, J. Haddad, and M. Ramezani, "Optimal perimeter control for two urban regions with macroscopic fundamental diagrams: A model predictive approach," *IEEE Trans. Intell. Transp. Syst.*, vol. 14, no. 1, pp. 348–359, Mar. 2013.

This article has been accepted for inclusion in a future issue of this journal. Content is final as presented, with the exception of pagination.

[12] M. Ramezani, J. Haddad, and N. Geroliminis, "Dynamics of heterogeneity in urban networks: Aggregated traffic modeling and hierarchical control," *Transp. Res. B, Methodol.*, vol. 74, pp. 1–19, Apr. 2015.
[13] M. Yildirimoglu, M. Ramezani, and N. Geroliminis, "Equilibrium analysis and route guidance in large-scale networks with MFD dynamics," *Transp. Res. Procedia*, vol. 59, pp. 404–420, Oct. 2015.
[14] S. Peeta and A. K. Ziliaskopoulos, "Foundations of dynamic traffic assignment: The past, the present and the future," *Netw. Spatial Econ.*, vol. 1, no. 3, pp. 233–265, Sep. 2001.
[15] H. Yang and S. Yagar, "Traffic assignment and signal control in saturated road networks," *Transp. Res. A, Policy Pract.*, vol. 29, no. 2, pp. 125–139, 1995.
[16] H. Ceylan and M. G. H. Bell, "Traffic signal timing optimisation based on genetic algorithm approach, including drivers' routing," *Transp. Res. B, Methodol.*, vol. 38, no. 4, pp. 329–342, 2004.
[17] F. Teklu, A. Sumalee, and D. Watling, "A genetic algorithm approach for optimizing traffic control signals considering routing," *Comput.-Aided Civil Infrastruct. Eng.*, vol. 22, no. 1, pp. 31–43, 2007.
[18] T. Le, H. Vu, Y. Nazarathy, Q. Vo, and S. Hoogendoorn, "Linear-quadratic model predictive control for urban traffic networks," *Transp. Res. C, Emerg. Technol.*, vol. 36, pp. 498–512, Nov. 2013.
[19] P. Varaiya, "Max pressure control of a network of signalized intersections," *Transp. Res. C, Emerg. Technol.*, vol. 36, pp. 177–195, Nov. 2013.
[20] C. F. Daganzo, "The cell transmission model: A dynamic representation of highway traffic consistent with the hydrodynamic theory," *Transp. Res. B, Methodol.*, vol. 28, no. 4, pp. 269–287, Aug. 1994.
[21] M. J. Lighthill and G. B. Whitham, "On kinematic waves. II. A theory of traffic flow on long crowded roads," *Proc. Roy. Soc. London A, Math. Phys. Sci.*, vol. 229, no. 1178, pp. 317–345, 1955.
[22] P. I. Richards, "Shock waves on the highway," *Oper. Res.*, vol. 4, no. 1, pp. 42–51, 1956.
[23] F. Zhu and S. V. Ukkusuri, "A linear programming formulation for autonomous intersection control within a dynamic traffic assignment and connected vehicle environment," *Transp. Res. C, Emerg. Technol.*, vol. 55, pp. 363–378, Jun. 2015.
[24] C. G. Prato, "Route choice modeling: Past, present and future research directions," *J. Choice Model.*, vol. 2, no. 1, pp. 65–100, 2009.
[25] C. M. J. Tampère, R. Corthout, D. Cattrysse, and L. H. Immers, "A generic class of first order node models for dynamic macroscopic simulation of traffic flows," *Transp. Res. B, Methodol.*, vol. 45, no. 1, pp. 289–309, 2011.
[26] Y. Han, Y. Yuan, A. Hegyi, and S. P. Hoogendoorn, "Linear quadratic MPC for integrated route guidance and ramp metering," in *Proc. IEEE 18th Intell. Transp. Syst. Conf. (ITSC)*, Sep. 2015, pp. 1150–1155.
[27] Y. Han, A. Hegyi, Y. Yuan, S. Hoogendoorn, M. Papageorgiou, and C. Roncoli, "Resolving freeway jam waves by discrete first-order model-based predictive control of variable speed limits," *Transp. Res. C, Emerg. Technol.*, vol. 77, pp. 405–420, Apr. 2017.
[28] M. Papageorgiou, "An integrated control approach for traffic corridors," *Transp. Res. C, Emerg. Technol.*, vol. 3, no. 1, pp. 19–30, 1995.
[29] A. A. Zaidi, B. Kulcsár, and H. Wymeersch, "Back-pressure traffic signal control with fixed and adaptive routing for urban vehicular networks," *IEEE Trans. Intell. Transp. Syst.*, vol. 17, no. 8, pp. 2134–2143, Aug. 2016.
[30] M. P. Dixon and L. Rilett, "Real-time OD estimation using automatic vehicle identification and traffic count data," *Comput.-Aided Civil Infrastruct. Eng.*, vol. 17, no. 1, pp. 7–21, 2002.
[31] A. Kotsialos, M. Papageorgiou, M. Mangeas, and H. Haj-Salem, "Coordinated and integrated control of motorway networks via non-linear optimal control," *Transp. Res. C, Emerg. Technol.*, vol. 10, no. 1, pp. 65–84, Feb. 2002.
[32] M. K. Kozlov, S. P. Tarasov, and L. G. Khachiyan, "The polynomial solvability of convex quadratic programming," *USSR Comput. Math. Math. Phys.*, vol. 20, no. 5, pp. 223–228, 1980.

Yu Han received the Ph.D. degree from the Delft University of Technology in 2017. He is currently a Data Scientist at Didi Chuxing Company, China. He is currently involved in the projects of implementing intersection signal control and ramp metering control in multiple cities in China. His research interests include road traffic flow modeling and road traffic control.

Andreas Hegyi (M'12) received the M.Sc. degree in electrical engineering and the Ph.D. degree from the Delft University of Technology (TU Delft), The Netherlands, in 1998 and 2004, respectively. From 2004 to 2007, he was a Post-Doctoral Researcher at TU Delft and Ghent University. He is currently an Assistant Professor at TU Delft. He has authored or co-authored over 100 papers. His research interests include traffic flow modeling and control, connected and cooperative vehicles, traffic state estimation, and traffic data analysis. He is a member of the IEEE-ITSS and IFAC-CTS. He has served as the Program Chair of the IEEE-ITSC 2013 Conference, as the General Chair of the IXth TRISTAN Symposium 2016, and as an IPC Member of various other conferences. He is an Associate Editor of the IEEE TRANSACTIONS ON INTELLIGENT TRANSPORTATION SYSTEMS and a member of the Editorial Board of *Transportation Research Part C*.

Yufei Yuan received the M.Sc. degree in transport and planning and the Ph.D. degree from the Delft University of Technology, The Netherlands, in 2008 and 2013, respectively. He is currently a fixed-term Researcher with the Delft University of Technology. During the past years, his research interests lie in traffic flow theory and simulation, data mining and processing, traffic state estimation and prediction, traffic management and analysis under evacuations, and intelligent transportation systems in general for fast vehicular traffic. His current research interests include slow traffic, including pedestrian and bicyclist flows, covering from modeling underpinning to simulation implementation.

Claudio Roncoli received the bachelor's degree, the M.Sc. degree in computer science engineering, and the Ph.D. degree in system monitoring and environmental risk management from the University of Genoa, Italy, in 2006, 2009, and 2013, respectively. He was a Research Assistant with the University of Genoa from 2007 to 2013 and a Visiting Research Assistant at Imperial College London, U.K., in 2011 and 2012. From 2013 to 2016, he was a Post-Doctoral Research Associate with the Technical University of Crete, Greece. Since 2016, he has been an Assistant Professor of transportation engineering with Aalto University, Finland, where he is currently an Assistant Professor of transportation engineering. He has authored over 40 papers published in international peer-reviewed journals, conference proceedings, and contributed books. His research interests include real-time traffic management, modeling, optimization, and control of traffic systems with connected and automated vehicles, and smart mobility and intelligent transportation systems.

Serge Hoogendoorn received the M.Sc. degree in applied mathematics and the Ph.D. degree in transport and planning from the Delft University of Technology, Delft, The Netherlands, in 1995 and 1999, respectively. He is currently the Chair Professor of traffic flow theory and management with the Department of Transport and Planning, Delft University of Technology. His research involves theory, modeling, and simulation of traffic and transportation networks, focusing on innovative approaches to collect detailed microscopic traffic data and the use of these data to underpin the models and theories.